A microbiota-directed complementary food intervention in 12-18-month-old Bangladeshi children improves linear growth

Ishita Mostafa MPH[1,5], Matthew C. Hibberd PhD[2,3,4], Steven J. Hartman BS[2,3,4], Md Hasan Hafizur Rahman MPH[1], Mustafa Mahfuz PhD[1,5], S. M. Tafsir Hasan MSc[1], Per Ashorn MD[5], Michael J. Barratt PhD[2,3,4], Tahmeed Ahmed PhD[1+], Jeffrey I. Gordon MD[2,3,4+*]

[1]International Centre for Diarrhoeal Disease Research, Bangladesh (icddr,b), Dhaka 1212, Bangladesh

[2]Edison Family Center for Genome Sciences and Systems Biology, Washington University School of Medicine, St. Louis, MO 63110 USA

[3]Center for Gut Microbiome and Nutrition Research, Washington University School of Medicine, St. Louis, MO 63110 USA

[4]Department of Pathology and Immunology, Washington University School of Medicine, St. Louis, MO 63110 USA

[5]Center for Child, Adolescent, and Maternal Health Research, Faculty of Medicine and Health Technology, Tampere University and Tampere University Hospital, Tampere, Finland

[+]Co-senior authors

*Address correspondence to:

Jeffrey I. Gordon MD
The Edison Family Center for Genome Sciences and Systems Biology
4515 McKinley Ave
St. Louis, MO 63110
Phone: 314-362-7243
jgordon@wustl.edu

SUMMARY

Background

Globally, stunting affects ~150 million children under five, while wasting affects nearly 50 million. Current interventions have had limited effectiveness in ameliorating long-term sequelae of undernutrition including stunting, cognitive deficits and immune dysfunction. Disrupted development of the gut microbiota has been linked to the pathogenesis of undernutrition, providing potentially new treatment approaches.

Methods

124 Bangladeshi children with moderate acute malnutrition (MAM) enrolled (at 12-18 months) in a previously reported 3-month RCT of a microbiota-directed complementary food (MDCF-2) were followed for two years. Weight and length were monitored by anthropometry, the abundances of bacterial strains were assessed by quantifying metagenome-assembled genomes (MAGs) in serially collected fecal samples and levels of growth-associated proteins were measured in plasma.

Findings

Children who had received MDCF-2 were significantly less stunted during follow-up than those who received a standard ready-to-use supplementary food (RUSF) [linear mixed-effects model, $\beta_{\text{treatment group x study week}}$ (95% CI) = 0.002 (0.001, 0.003); P=0.004]. They also had elevated fecal abundances of *Agathobacter faecis*, *Blautia massiliensis*, *Lachnospira* and *Dialister*, plus increased levels of a group of 37 plasma proteins (linear model; FDR-adjusted P<0.1), including IGF-1, neurotrophin receptor NTRK2 and multiple proteins linked to musculoskeletal and CNS development, that persisted for 6-months post-intervention.

Interpretation

MDCF-2 treatment of Bangladeshi children with MAM, which produced significant improvements in wasting during intervention, also reduced stunting during follow-up. These results suggest that the effectiveness of supplementary foods for undernutrition may be improved by including ingredients that sponsor healthy microbiota-host co-development.

Funding

This work was supported by the BMGF (Grants OPP1134649/INV-000247).

ClinicalTrials.gov identifier: NCT04015999

Introduction

Childhood undernutrition is a public health priority manifested by impaired ponderal and linear growth (wasting and stunting), immune and metabolic dysfunction, altered central nervous system (CNS) development as well as other physiologic abnormalities[1]. Undernutrition is typically classified using anthropometric assessments. It is estimated that globally, ~50 million children under the age of five suffer from acute malnutrition (wasting); those with moderate acute malnutrition (MAM) have weight-for-length Z scores (WLZ) that are 2-3 standard deviations below the median (WLZ -2 to -3) of a reference multi-national cohort of children with healthy growth, while WLZ <-3 is characteristic of those with non-oedematous severe acute malnutrition (SAM)[2]. Stunting is the most prevalent form of childhood malnutrition, affecting around 150 million children with nearly one in three afflicted in parts of South Asia and sub-Saharan Africa[3]. Stunting often begins prenatally and is linked to maternal risk factors (height, age, education); after birth, it may continue to worsen under the influence of environmental stressors (e.g. poor diet, infection) until at least 2-years-of-age, whereafter LAZ scores remain low for children in many low-income countries[4-6]. Children under-5 who are stunted are five times more likely to die than non-stunted children and those who survive may suffer impairments in immune and cognitive development and have increased risk for chronic illnesses in adult life[7,8].

Wasting and stunting are typically treated differently. Wasting is treated with high energy micronutrient-fortified ready-to-use supplementary or therapeutic foods (RUSF/RUTF) in the community or in hospital-based settings[9,10]. Approaches to treating stunting have been multifaceted, including strategies to reduce enteropathogen burden and environmental enteric dysfunction (EED)[11] through access to clean water, sanitation, and improved hygiene (WASH), as well as various maternal, infant and young child feeding programs. To date evidence for the relative effectiveness of these approaches has been mixed[12,13]. Moreover, wasting and stunting frequently co-exist in the same infant/child, either concurrently or at different periods in their development, with co-occurrence being more common in severely wasted children and associated with significantly greater risk of mortality compared to either form of undernutrition alone[14-16]. Analyses of longitudinal studies of infant growth in the U.S., Honduras, Ghana and Malawi have found that weight gain in a preceding 3-month interval is associated with linear growth in the following interval[17,18]. A major challenge in interpreting these results is the lack of deeper knowledge of the underlying physiologic changes that occur within a given individual over time, and how these changes are related mechanistically to their growth trajectories.

Given the modest effectiveness of existing interventions, efforts are being made to obtain a more comprehensive view of the biological state or states associated with undernutrition, gather new insights into pathogenesis and identify additional therapeutic targets. One outcome of these efforts is recognition of the contributions of the gut microbiota. Birth cohort studies have disclosed that

children with undernutrition have impaired postnatal development of their gut microbial communities compared to their age-matched healthy counterparts. This impaired development (microbiota immaturity) is worse in children with SAM compared to those with MAM and is not repaired by standard therapeutic food[19-21]. Phenotypic comparisons of gnotobiotic mice colonized with fecal microbiota from age-matched healthy children or those with wasting and stunting have revealed bacterial strains whose abundances/expressed functions are higher in healthy microbiota and that are able to ameliorate growth faltering when added to mice colonized with the microbiota from undernourished children[22].

Based on these findings, gnotobiotic mice were used to 'screen' complementary foods commonly consumed in Bangladesh to test whether any had the ability to increase the fitness/expressed beneficial functions of growth associated taxa that are underrepresented during the weaning period in the microbiota of undernourished Bangladeshi children compared to their healthy counterparts. This effort ultimately led to the development of a 'microbiota-directed complementary food' prototype ('MDCF-2'), containing 'microbiota-active' ingredients - chickpea, soy flour, peanut paste and green banana - along with vegetable oil, sugar and micronutrients[23]. A 3-month randomized controlled trial of MDCF-2 in 12-18-month-old Bangladeshi children with MAM revealed that children who received a MDCF-2 had a significantly greater rate of weight gain (WLZ) compared to children who received a standard RUSF, despite the fact that MDCF-2 had a 15% lower caloric density than the RUSF[24,25]. The superiority of MDCF-2 was linked to changes in the abundances of bacterial strains (metagenome-assembled genomes, MAGs) including strains of *Prevotella copri* that were significantly associated with improved WLZ and which possessed a distinct repertoire of polysaccharide utilization loci (PULs) compared to non-WLZ-associated *P. copri* MAGs[26]. The superior ponderal growth of children treated with MDCF-2 was accompanied by increases in the levels of plasma proteins that are biomarkers and mediators of musculoskeletal growth and neurodevelopment, plus decreases in the levels of plasma proteins that are biomarkers and mediators of inflammation[25]. Nonetheless, at the end of the 3-month intervention, children treated with MDCF-2 did not show statistically significant differences in their LAZ scores compared to those who received RUSF.

In this report, we describe the results of a 2-year follow-up of these children, which included anthropometry and assessment of the fecal microbiota and plasma proteome. Our results reveal that 3-months of MDCF-2 treatment not only provides a rapid and sustained improvement in ponderal growth, but also leads to superior linear growth in the follow-up period compared to RUSF. These findings, together with corresponding changes in the representation of growth associated MAGs and levels of plasma proteins involved in various facets of growth, provide evidence that the benefits of MDCF-2 treatment extend beyond the period of its administration in this population of Bangladeshi children with MAM.

RESEARCH IN CONTEXT

Evidence before this study

Undernutrition is the leading cause of death of children under 5-years-of-age worldwide. This multifaceted global health challenge is expected to become more severe in part due to intersecting effects of climate change, increasing economic disparities affecting low- and middle-income countries (LMICs), and continued geopolitical upheaval. Undernutrition not only increases the risk of death but is also associated with persistent sequelae including stunting, immune dysfunction, and cognitive deficits. Numerous epidemiologic studies have shown that undernutrition is not due to food insecurity alone. Moreover, current nutritional interventions, while reducing mortality, have had limited success in overcoming these sequelae.

Added value of this study

We performed a 3-month randomized controlled trial in which a microbiota-directed complementary food formulation (MDCF) was compared to a standard RUSF in 12-18-month-old Bangladeshi children with MAM, who were also stunted. We previously reported that supplementation with MDCF improved ponderal growth compared to RUSF, despite the fact that the latter was more calorically dense. Here we report the results of a 2-year follow-up of these children which revealed significantly better LAZ scores in MDCF-2 compared to RUSF-treated children that was manifested only during the follow-up period. Improved LAZ was accompanied by significant differences in the representation of growth-associated bacterial taxa, plus significant elevations in plasma protein mediators/biomarkers of musculoskeletal growth and neurodevelopment that extended beyond the period of intervention.

Implications of all the available evidence

Children with MAM and SAM have perturbed gut microbial community development that is manifested by alterations in the representation of growth-associated bacterial taxa as well as microbial genes comprising various metabolic pathways. The result of these perturbations are microbial communities whose configurations resemble those of chronologically younger children. Standard nutritional interventions in children do not fully repair these perturbed community states. Our findings suggest that microbiota-directed foods, designed to improve the representation and/or expressed metabolic functions of key gut bacteria, not only improve weight gain but also linear growth and plasma biomarkers of a range of developmental processes. These findings set the stage for additional studies to determine (i) the extent to which linear growth benefits of MDCF-2 are manifested in stunted children who are not also wasted; (ii) whether the observed plasma biomarker signatures/responses to MDCF-2 foreshadow clinical improvements in body composition and cognitive performance, and (iii) optimal conditions for initiating treatment (e.g., age, severity of undernutrition, MDCF dose/duration). Deeper knowledge of these relationships may enable an

evolution in policies for treating undernourished children beyond current recommendations that are based largely on considerations of the energy density and macro-/micronutrient content of diets and therapeutic foods.

METHODS

Human study design

The study design for the randomized controlled trial comparing the efficacy of a microbiota-directed complementary food (MDCF-2) and a ready to use supplementary food (RUSF) in promoting weight gain in 12-18-month-old Bangladeshi children with MAM is shown in **Fig 1a**. The clinical study (ClinicalTrials.gov identifier:NCT04015999) was conducted in the Mirpur slum of Dhaka, Bangladesh from December, 2018 to October, 2019 as previously described[24,25] The protocol was approved by the ethics review committee at the International Centre for Diarrhoeal Disease Research, Bangladesh (icddr,b). Children were screened and enrolled through household surveys in the community by Field Research Assistants and written consent was obtained from the parents of the study participants. Eligible children (male and female) with MAM (WLZ -2 to -3) who met the inclusion criteria were enrolled and randomly assigned to receive either a rice, lentil, milk powder, sugar and soybean oil-based RUSF, or MDCF-2, which contains chickpea flour, soy flour, peanut and green banana plus soybean oil and sugar. A total of 124 children were enrolled (n=62/arm)[24]. At enrollment (baseline), anthropometric assessments were performed, and fecal and plasma samples were collected from each child. MDCF-2 and RUSF, freshly prepared at the icddr,b Food Processing Facility located in Mirpur were provided to participants twice daily for 3 months under supervision by trained study staff (morning and afternoon, 2 x 25g servings/day). The total energy provided by the supplements was 220-250kcal/day or ~20-25% of the daily recommended energy intake (and 70% of the recommended micronutrients) for healthy 12–18-month-old children. Caregivers were instructed not to feed their children during the 2-hour period before each visit; otherwise, their usual breastfeeding and complementary feeding practices were maintained. Fecal specimens were collected prior to intervention, weekly during the 1st month of intervention, and every 4 weeks during the second and third month of intervention. After cessation of the intervention, fecal sampling was performed at the 1, 6 and 12 months of follow-up. (Note that these follow-up time points relate to the end of *study months* 4, 9 and 15 respectively; **Fig. 1a)**. Blood samples were collected prior to intervention, at the end of first and third month of intervention, and at 1, 6 and 12 months of follow-up.

Anthropometric assessments were performed by trained field research assistants at enrollment (just prior to treatment), every 15 days during the intervention period, 1 month after cessation of treatment and at 9, 15, 21 and 27 months after enrollment into the study. The presence/absence of any illness during the 7 days preceding each anthropometric assessment was recorded. The weight of each child was determined using a digital scale with 2 g precision (Seca, model 728, Germany). Length was measured using an infantometer (Seca, model 416, Germany), and mid-upper arm circumference (MUAC) was determined to the nearest millimeter (using a non-stretch tape). Each measurement was taken twice at a single timepoint by two separate individuals and the average score was recorded. Z

scores were calculated using the new child growth standards of the World Health Organization (WHO)[2]. For each of the four main anthropometric assessments, we modeled the treatment group-specific trajectories using the following linear mixed effects model:

$$anthropometric\ assessment \sim \beta_1(week\ after\ treatment) + \beta_2(age\ at\ baseline) + \beta_3(sex) + \beta_4(illness\ in\ prior\ seven\ days) + (1|participant) \quad (1)$$

We employed the model below to compare effects between the treatment groups:

$$anthropometric\ assessment \sim \beta_1(treatment\ group\ x\ week\ after\ treatment) + \beta_2(age\ at\ baseline) + \beta_3(sex) + \beta_4(illness\ in\ prior\ seven\ days) + \beta_5(treatment\ group) + \beta_6(week\ after\ treatment) + (1|participant) \quad (2)$$

Biospecimen collection

Fecal and plasma specimens were collected as previously described[25]. In brief, within 20 minutes of defecation, aliquots of the fecal sample were transferred by the field worker into sterile 2 mL cryovials and transferred into cryo-shippers (Taylor Wharton/ Worthington Industries CX300) that had been pre-charged with liquid nitrogen. Cryo-shippers were transported to the study center where their contents were recorded, and the vials transferred to a -80°C freezer. Venous blood was collected in EDTA-plasma tubes; plasma recovered after centrifugation (3000 x g for 10 minutes at room temperature) was aliquoted into cryovials and stored at -80°C. Specimens were shipped to Washington University in St Louis USA on dry ice and stored at -80°C in a dedicated biospecimen repository prior to analysis, with approval from the Washington University Human Research Protection Office. For this study, 225 fecal samples (n=114 at 6 months follow-up and n=111 at 12 months) and 219 plasma samples (n=111 at 6 months follow-up and n=108 at 12 months) were collected/analyzed. Additional fecal and plasma samples included in the analyses described here were collected prior to, during and at the end of the intervention, plus at the 1-month follow-up time point, as previously reported[25,28].

Quantification of enteropathogens by multiplex qPCR

The same qPCR assay employed in the treatment phase of the study was applied in the post-treatment follow-up phase to measure 23 bacterial, viral and protozoan enteropathogens[25-27]. Enteropathogen abundances were compared between the treatment groups at the end of treatment, and at 6- and 12-months post-treatment using both Kruskal-Wallis tests applied to log_{10}-transformed enteropathogen abundances at each sampling timepoint and linear, mixed-effects models of the following form:

$$log_{10}(enteropathogen\ abundance) \sim \beta_1(age\ at\ sampling) + \beta_2(sex) + \beta_3(study\ week) + \beta_4(treatment\ group) + \beta_5(study\ week{:}\ treatment\ group) + (1|participant)\#(3)$$

$$log_{10}(enteropathogen\ abundance) \sim \beta_1(age\ at\ sampling) + \beta_2(sex) + \beta_3(illness\ in\ prior\ seven\ days) + \beta_4(study\ week) + \beta_5(treatment\ group) + (1|participant) \#(4)$$

Significance for the Kruskal-Wallis test, Eq. 3 (β_5 term) and Eq. 4 (β_3 term) was defined by $q<0.05$ (*P-value* adjusted to control for multiple hypotheses using the Benjamini-Hochberg correction[29]).

Isolation and short-read shotgun sequencing of fecal DNA

DNA was isolated from 225 fecal samples representing the 6- and 12- month post-treatment follow-up timepoints as previously described[28] and shotgun metagenomic sequencing libraries were prepared with a modified Nextera XT (Illumina) protocol[30]. Libraries were quantified, balanced, pooled, and sequenced to a depth of $8.96x10^7 \pm 2.09x10^7$ 150 nt paired-end reads/sample (mean±SD) at similar scale and on the same Illumina NovaSeq 6000 sequencing platform (S4 flow cell) as the treatment phase fecal metagenomic sequencing effort described previously[28]. [Negative (water only) process controls were included in both the treatment phase and follow-up sequencing efforts. Library preparation and sequencing of these samples yielded $6.70x10^4 \pm 3.01x10^4$ (mean±SD) reads]. Reads were demultiplexed and pre-processed to remove low-quality bases/reads, as well as reads mapping to the hg19 assembly of the human genome[28].

Quantitation of Abundances of Metagenome Assembled Genomes (MAGs)

Pre-processed shotgun data from the 6- and 12- month follow-up time points were mapped using Kallisto (v0.43.0)[31] to a single quantification index from the set of 1,000 high-quality MAGs (completeness ≥90%, contamination <5%) generated from data collected during the treatment phase and 1 month follow-up time point of this study[28]. The 1,000 MAGs were produced using an assembly strategy in which shotgun sequencing reads generated from fecal samples serially collected from a given trial participant were aggregated and assembled into a 'participant-specific' MAG set. MAGs from all participants were then compared and dereplicated to generate a set of study-wide MAGs. MAGs were considered redundant if they shared 99% average nucleotide identity (ANI)[28]. Taxonomy was subsequently assigned to these MAGs using a consensus approach based on (i) Kraken (v2.0.8)[32] and Bracken (v2.5)[33] plus (ii) the Genome Taxonomy Database Toolkit (GTDB-tk)[34] and GTDB database (v0.95). We then mapped fecal shotgun sequencing data from the additional follow-up time points to the 1,000 MAGs assembled previously to facilitate the merging of the datasets. After merging, the dataset contained abundance data for each of the 1,000 MAGs across 928 samples (703 samples representing the period from pretreatment through 1 month of follow-up[28] and 225 from the 6- and 12-month follow-up time points) with matching anthropometric assessments. This dataset was then filtered to exclude MAGs below a threshold count of 5 reads per kilobase per million in ≥ 40 % of samples, yielding a final dataset containing 851 MAGs.

Principal components analysis

We assayed the stability of the microbiota over the first 12 months of post-intervention follow-up using principal components analysis (PCA) applied to the filtered, VST-transformed dataset spanning treatment and follow-up samples described above. PCA was performed using the 'prcomp' function in R (v4.3.2); sample projections and information regarding variance explained by each principal component (PC) were extracted as previously described[28]. PCs explaining variance above 'background' were correlated to the age at which each fecal sample was collected (Pearson) (background defined by applying PCA to a permuted dataset[28]). PC projections were compared over time and between treatment groups using t-tests, with statistical significance defined as *P*-value < 0.05.

Identifying MAGs and MAG features associated with MDCF-2 treatment and/or anthropometric recovery

We used linear mixed effects modeling (dream, part of the variancePartition package v1.24.1, in R v4.3.2)[35] to relate the untransformed abundances of MAGs to 'treatment group', 'weeks after intervention' and the interaction of these terms, while controlling for repeated sampling from each participant:

$$MAG\ abundance \sim \beta_1(sex) + \beta_2(age\ at\ sampling) + \beta_3(treatment\ group) + \beta_4(weeks\ after\ intervention) + \beta_5(treament\ group\ x\ weeks\ after\ intervention) + (1|participant) \#(5)$$

This model was applied to the abundance dataset containing 851 MAGs in fecal samples collected at the end of treatment plus 1, 6, and 12 months into the post-intervention follow-up (defined in the model as 12, 16, 36 and 60 weeks from the start of the trial). Relationships between MAG abundances and terms in the model were considered significant if they displayed q<0.05.

We employed gene set enrichment analyses (GSEA; fgsea v3.14)[36] to identify similar abundance responses in the set of 75 positively or 147 negatively WLZ-associated MAGs identified in our prior analyses of treatment-phase fecal samples[28]. MAGs were ranked based on a standardized z statistic describing their relationship with terms from the linear mixed effects model described in Eq. 5 above, after which GSEA was performed. Sets of MAGs displaying q<0.05 were considered significant.

We also performed a differential abundance analysis of MAGs between the MDCF-2 and RUSF treatment groups at each time point using a simplified model (dream, v1.24.1) relating MAG abundance only to the treatment group, with significant differences between groups defined as having a q<0.05. Enrichment analyses for the positively or negatively WLZ-associated MAGs were also applied to comparisons of MAG abundances at each time point using the methods and statistical criteria described above.

To identify MAGs whose abundances were associated with the rate of change in LAZ in the follow-up phase, we transformed the filtered MAG abundance dataset using the Variance Stabilizing Transformation (VST)[37]; we then filtered this dataset to the timeframe spanning the end of treatment and 12-months of follow-up and determined relationships with LAZ using the following model:

$$LAZ \sim \beta_1(sex) + \beta_2(age\ at\ sampling) + \beta_3(VST - transformed\ MAG\ abundance) + \beta_4(weeks\ after\ intervention) + \beta_5(VST - trans.\ MAG\ abundance\ x\ weeks\ after\ intervention) + (1|participant)\#(6)$$

Statistical significance was determined for the β_3 term using ANOVA with a cutoff of $q<0.05$. We additionally used the β_3 coefficients corresponding to each MAG abundance relationship with LAZ as a ranking factor for GSEA, after which sets of MAGs, grouped by (i) species-level taxonomic assignment, (ii) WLZ-association in the treatment phase and (iii) the presence or absence of encoded metabolic pathways were tested for enrichment (significant enrichments were indicated by $q<0.05$). Metabolic pathway annotations for MAGs were based on alignment to the mcSEED database and *in silico* prediction of pathway presence/absence as previously described[28].

Aptamer-based plasma proteomic analysis

The SomaScan proteomic assay plasma/serum kit (SomaLogic, v4.0) was used as previously described[25] to quantify 5,284 proteins in the plasma samples that had been collected from study participants at enrollment and 1, 3, 9 and 15 months after enrollment. Plasma samples were separated into two batches for data acquisition, with the first consisting of samples collected at enrollment, 1- and 3-months (treatment phase), and the latter from 9- and 15-months (follow-up). Each 50 µL aliquot of plasma was incubated with NHS-biotin-tagged aptamer probes ('SOMAmers') to form protein-specific SOMAmer complexes. After immobilization on streptavidin beads, complexes were cleaved, denatured, eluted, and hybridized to customized Agilent DNA microarrays. Arrays were scanned (Agilent SureScan; 5 µm resolution) and the Cy3 fluorescence signal processed using SomaLogic's standardization procedures[25]. Protein abundances were $\log_2$-transformed prior to analysis.

To assess whether the 75 plasma proteins that were associated with the rate of weight gain (β-WLZ) in the treatment phase[25] were also predictive of the rate of change in WLZ or LAZ during the follow-up period, we first calculated the rate of change of these 75 proteins during treatment (0-3 months) for each participant in each treatment arm [n=113 samples at enrollment, n=114 at the end of treatment]. Next, we calculated the rate of change in WLZ and LAZ in each participant during the follow-up period (months 3-27) and used linear models to relate the rate of change of each protein during treatment to the rate of change of LAZ or WLZ during the follow-up period:

$$slope(WLZ\ follow\text{-}up) \sim \beta_1(slope(protein\ levels\ treatment\ phase)) + \beta_2(age\ at\ enrollment) + \beta_3(sex) \quad (7)$$

and

$$slope(LAZ\ follow\text{-}up) \sim \beta_1(slope(protein\ levels\ treatment\ phase)) + \beta_2(age\ at\ enrollment) + \beta_3(sex) \quad (8)$$

Significance was assigned after correcting for multiple testing for each anthropometric measure ($q<0.1$).

We applied a linear mixed effects model to test whether any of the proteins significantly associated with anthropometric changes (as defined from Eq. 7 and 8) exhibited a greater rate of change in one or other treatment group during the treatment phase:

$$protein\ abundance \sim \beta_1(study\ week) + \beta_2(treatment\ group) + \beta_3(study\ week{:}treatment\ group) + (1|participant) \quad (9)$$

ANOVA was used to test for statistical significance, with correction for multiple testing ($q<0.1$). To determine if the resulting proteins were significantly associated with a treatment group as a whole, we applied a one-way t-test to the β_3(study week:treatment group) coefficients collected for each protein.

For plasma samples collected at the 6- and 12-month follow-up time points [n=111 samples at month 6 and n=108 at month 12], a linear model was applied to identify LAZ-associated plasma proteins whose levels were differentially abundant between the two treatment arms at each time point:

$$protein\ abundance \sim \beta_1(treatment\ group) \quad (10)$$

We applied a one-way t-test to the β_1(treatment group) coefficients for proteins at the 6- and 12-month follow-up time points and subsequently applied a false-discovery rate correction on the *P*-values obtained from the t-tests applied to Eq. 9 β_3 and Eq. 10 β_1 coefficients ($q<0.05$).

Illness and dietary intake during the follow-up period

Each child was monitored for illness daily for one continuous week ending at or near the time of anthropometry data collection at the end of treatment and at the end of 1, 6, 12, 18, and 24 months of post-intervention follow-up. Food frequency questionnaires were administered at the same time points and used to calculate Minimum Acceptable Diet (MAD) per World Health Organization and UNICEF guidelines[38]. MAD is only valid for children 6-23 months old. Children in our clinical trial surpassed this range between 1- and 6-months of post-intervention follow-up. Therefore, we applied chi-squared tests comparing whether MAD criteria were met for the MDCF-2 versus the RUSF treatment groups at the 1- and 6-month follow-up timepoints. Significance was defined by $P<0.05$.

Role of the funding source

The funders of this work were not involved in designing the study or in the collection, analysis, interpretation of the data, and did not participate in writing the manuscript.

RESULTS

Anthropometric recovery of children with MAM during and after treatment with MDCF-2

Out of 124 children, 118 (n=59/arm) completed the intervention; their anthropometric characteristics at the end of the treatment phase (i.e., the beginning of follow-up) are shown in **Table 1.** For each time point of anthropometric assessment (**Figure 1a**), we modeled the treatment group-specific trajectories as well as differences between groups using linear mixed effects models, controlling for, treatment time, age, sex and the presence of any illnesses in the 7 days prior to anthropometry (see *Methods,* Eq. 1 and 2; **Supplementary Table S1A,B**). The superior WLZ achieved by children in the MDCF-2 arm at the end of treatment (**Figure 1b**) was maintained through follow-up, though the difference in rate of change of WLZ between the groups was no longer significant (P=0.22; linear mixed effects model) (**Figure 1c; Supplementary Table S1B**). Weight-for-age (WAZ) also trended higher in the follow-up period for MDCF-2 treated children, although this difference was not statistically significant (**Supplementary Table S1B**).

Linear growth faltering often begins *in utero* and may continue to worsen during the first 2 postnatal years in low-income countries such as Bangladesh[4]. In our randomized controlled trial, LAZ was not different between the two groups during the treatment phase (P=0.6 linear mixed effects model**; Figure 1d, Supplementary Table S1A**). However, in the 24-month post-intervention follow-up period (**Table 2**), we observed a statistically significant decrease in the rate of LAZ decline in children that had received 3 months of MDCF-2 supplementation compared to those that had received RUSF (P=0.004; **Figure 1e; Supplementary Table S1B**). To examine whether differences in the quality of diets consumed by children in the follow-up period may have contributed to differences in linear growth trajectories between the intervention groups, we examined food frequency data collected during follow-up period and compared the Minimum Acceptable Diet (MAD) scores for each group. MAD is an indicator of infant and young child feeding (IYCF) practices for 6-23-month-old children that is used to describe the quality of a child's diet and is defined as the percentage of children (in the 6–23-month age range) who consumed a minimum acceptable diet during the previous day[38]. MAD was not significantly different between the MDCF-2 and RUSF groups at the 1- and 6-month follow-up time points when this measurement was applicable based on age (chi-squared P>0.05, **Supplementary Table S1C**). Taken together, these results indicate that compared to the more calorically dense RUSF used in this RCT of children with MAM, a relatively short intervention with MDCF-2 provided improvements not only in their ponderal growth, but also a sustained difference in linear growth that is not explained by differences in quality of diet consumed by children during follow-up.

Effects of MDCF-2 on the microbiota

We next assessed whether the improvements in anthropometry during the follow-up period were associated with durable changes in the microbiota resulting from treatment with MDCF-2. Of the 118 children who completed the intervention, we collected fecal samples from 114 after 6 months of follow up (n=57/treatment group), and 111 at 12 months (n=56, MDCF-2 treatment group; n=55, RUSF treatment group) (i.e., there was only 6% loss to follow-up at 12 months).

We employed a qPCR assay[25] to quantify the abundances of 23 bacterial, viral and protozoan enteropathogens in each child's fecal samples (**Supplementary Table S2A**). Neither pairwise comparisons of enteropathogen abundances, nor the total number of detected enteropathogens at the cessation of treatment, or at 6- or 12-months post-treatment revealed any significant differences between the treatment groups (Kruskal-Wallis tests, $q>0.05$). Likewise, linear mixed-effects models designed to identify the effects of interactions between treatment group and time after cessation of treatment (controlling for age and sex) on enteropathogen abundances failed to identify significant differences between the treatment groups (**Supplementary Table S2B**). We subsequently examined the relationship between the enteropathogen levels and illnesses reported in the seven days prior to fecal sample collection; these analyses revealed a significant positive relationship between diarrheal illness and (i) the total number of enteropathogens detected and (ii) the abundances of *C. jejuni*, enterotoxigenic *E. coli*, Cryptosporidium and diarrheal illness, independent of age, sex, timepoint or treatment group (**Supplementary Table S2C**).

To analyze the fecal microbial communities of MDCF-2- and RUSF-treated participants sampled during the post-intervention follow-up period, we mapped shotgun sequencing data generated from fecal samples collected at the 6- and 12-month follow-up timepoints to the set of 1,000 high-quality metagenome assembled genomes (MAGs) assembled from fecal shotgun sequencing data collected during the treatment phase of the study[28]. These datasets were merged with data generated from the treatment phase of the study and one-month follow-up, after which filtering was applied to exclude sparsely represented MAGs. This effort resulted in a dataset comprising 851 MAGs across 928 samples with matched anthropometry data (see *Methods*).

We applied a principal components analysis (PCA) to the full MAG dataset spanning pretreatment through 12 months of follow-up. We identified principal components (PCs) that explained variance above background (*Methods*). PC1, explaining 19.2% of variance, was significantly correlated with a child's age at the time of sample collection (Pearson $P<2.2\text{x}10^{-16}$). We therefore used the projection of each sample along PC1 as a dimensionality-reduced metric of microbiota 'age'. As expected, given that the treatment and early follow-up phases of the study occurred in children at an age when the microbiota is developing[19], there was a significant change in position along PC1 between samples collected at 1 and 6 months and 6 and 12 months of follow-up ($P=1.87\text{x}10^{-9}$ and $P= 6.43\text{x}10^{-7}$, respectively; t-test). However, we observed no significant difference

between the PC1 projections of samples obtained from participants in the MDCF-2 and RUSF arms during the follow-up phase, when children were between 16- and 33-months-old (P>0.05, t-tests).

We proceeded to analyze the abundances of each individual MAG over time during the period between the end of treatment and 12 months of follow-up in children formerly treated with MDCF-2 or RUSF. As in the treatment phase, no single MAG met our criteria for statistically significant differential abundance or differential rate of change of abundance between the two treatment groups during this period (q>0.05, linear mixed effects model, Eq. 5; **Supplementary Table S3A**). However, employing gene set enrichment analysis (GSEA), we compared the representation of the MAGs previously identified[28] as significantly positively (n=75) or negatively (n=147) associated with WLZ during the treatment phase, in fecal samples obtained at the end of treatment and at 1, 6 and 12 months of follow-up. MAGs that were positively associated with WLZ were enriched in the MDCF-2 treatment group, while MAGs that were negatively associated with WLZ were enriched in the RUSF group at the end of treatment, and at one month of follow-up (GSEA q<0.05, (**Fig. 2a**, **Supplementary Table S3C,D**). The enrichment of positively WLZ-associated MAGs was driven by 15 MAGs assigned to the species *Agathobacter rectalis* (5 MAGs), *Blautia massiliensis* (5 MAGs), *CAG-217 sp00436335* (family Acutalibacteraceae, 2 MAGs), *ER4 sp000765235* (family Oscillospiraceae, 2 MAGs), *Parolsenella catena* (2 MAGs), and *Prevotella copri* (2 MAGs; **Fig. 2b**). Notably, these two *P. copri* MAGs were Bg0018 and Bg0019 – both positively associated with WLZ - that express polysaccharide utilization loci involved in the metabolism of glycans enriched in MDCF-2 compared to RUSF[28]. The enrichment of this set of 15 MAGS was no longer statistically significant at the 6-month post-intervention time point (GSEA q>0.05).

Given the effect of prior MDCF-2 treatment on LAZ in the follow-up period, we initially used the same approach we had employed to identify WLZ-associated MAGs to search for LAZ-associated MAGs in the follow-up phase. Our efforts to model the relationship between MAG abundance and LAZ yielded only one significantly associated MAG, Bg0899, which was negatively associated and classified within the family Lachnospiraceae (q<0.05, linear mixed effects model (Eq.4), **Supplementary Table S3E**). Therefore, we expanded this analysis by ranking MAGs based on the coefficient describing their relationship with LAZ over time in the follow-up period [β_3(MAG abundance x weeks after intervention)] and applying GSEA to sets of MAGs defined by their species assignments. Using this approach, we identified a group of four species (*Agathobacter faecis*, *Blautia massiliensis*, *Lachnospira sp000436475* and *Dialister sp000434475* and) that were positively associated with LAZ (q<0.05, GSEA, **Supplementary Table S3F**). *Agathobacter* produce the beneficial short chain fatty acid (SCFA) butyrate though fermentation of mono- di- and oligo-saccharides[39], while *Blautia massiliensis* is reported to be enriched in carbohydrate transport and metabolism capacities compared with other species in the genus *Blautia*, with acetate a key product of

fermentation[40,41]. *Lachnospira* and *Dialister* also contribute to the fermentation of carbohydrates and production of SCFA.

Finally, we looked for relationships between MAGs that were significantly associated with WLZ in the treatment and follow-up phases of the trial. This analysis revealed a group of 75 MAGs positively correlated with WLZ in the treatment phase[28] that were also enriched among LAZ correlated MAGs during follow-up ($q=1.24x10^{-4}$, GSEA applied to MAGs ranked by their LAZ association; **Supplementary Table S3G**). Notably, the 25 MAGs that had the strongest associations with both LAZ and WLZ were predominantly assigned to the families Lachnospiraceae (n=12 MAGs), Ruminococcaceae (n=8) or Oscillospiraceae (n=3) (**Supplementary Table S3H**). An analysis of MAGs whose abundances were positively associated with LAZ yielded no significantly enriched metabolic pathways (GSEA, $q>0.05$). However, DNA abundance is an imprecise proxy for functional activity and additional analyses involving microbial RNA-Seq are required to characterize the relationship between *expressed* community functions influenced by MDCF-2 and linear growth.

Effects of MDCF-2 on the plasma proteome

We next sought to determine whether the plasma proteins positively (n=70) or negatively (n=5) associated with improvements in weight gain (β-WLZ) during the treatment phase [n=113 plasma samples analyzed at enrollment and n=114 at the end of treatment][25] were also associated with the rate of change in either WLZ or LAZ during follow-up. We used linear models, accounting for age and sex (Eq. 7,8) to regress the rate of change of each of the 75 proteins to the rate of change of WLZ or LAZ during the 24-month follow-up phase. This analysis disclosed that while none of the proteins remained significantly associated with ponderal growth (WLZ) (**Supplementary Table S4A**), 37 were significantly positively associated with rate of change of LAZ during follow-up ($q< 0.1$, **Fig. 3a Supplementary Table S4B**); all of these were positively associated with WLZ during the treatment phase[25]. They include biomarkers/mediators of musculoskeletal development; e.g., cell adhesion molecule-related/down-regulated by oncogenes (CDON) which is a positive regulator of myogenesis[42], dermatopontin (DPT) which accelerates collagen fibrillogenesis[43], thrombospondins-3 and -4 (THBS3,4) which are involved in tissue remodeling and skeletal maturation via interaction with the extracellular matrix[44,45], plus a number of collagens (e.g., COL15A1, COL9A1, COL6A3). Other notable proteins among the 37 positively associated with LAZ include insulin-like growth factor-1 (IGF-1) which acts in concert with growth hormone to control linear growth in children[46] and a Wnt inhibitor, secreted frizzled-related protein 4 (SFRP4), involved in formation of bone cortex[47]. The list also includes effectors of CNS development: e.g., RET which encodes the receptor tyrosine kinase for glial cell derived neurotrophic factor (GDNF)[48]; the axon guidance protein SLIT and NTRK like family member 5 (SLITRK5)[49], BDNF/NT-3 growth factors receptor (NTRK2) which is involved in synaptogenesis and learning and memory[50], plus roundabout homolog 2 (ROBO2), an axon

guidance receptor recently reported to also promote osteoblast differentiation and mineralization[51] (see **Fig. 3b** for complete list of these proteins and their functional annotations).

For each of the 37 LAZ-associated proteins, we applied a linear mixed-effects model (Eq. 9 in *Methods*) to obtain their differential rates of change in levels during the treatment phase between the MDCF-2 and RUSF groups (**Supplementary Table S4C**). A one-way t-test was then performed on the β_3*(month:treatment group)* coefficients; each coefficient represents the differential rate of change in the level of each protein between the two groups during treatment. The analysis revealed that these proteins, as a group, were significantly enriched in the MDCF-2 arm (FDR corrected $q<0.05$; **Fig 3c**). We next used a linear model (Eq. 10 in *Methods*) to test whether the LAZ-associated proteins were differentially abundant between the MDCF-2 and RUSF treatment arms at month 6 and month 12 of the follow-up period [n=111 plasma samples analyzed at the end of month 6; n=108 at the end of month 12] (**Supplementary Table S4D,E**). While none of the 37 proteins exhibited significant differences in their levels between treatment arms at either follow-up time point ($q>0.1$), as a group their levels in plasma was significantly higher in MDCF-2 compared to RUSF treated children at the 6-month follow-up time point [(one-way t-test applied to the β_1*(treatment group)* coefficients in Eq. 10 with $q<0.05$ (**Fig. 3c**)]. By 12 months of follow-up, this enrichment was no longer evident. Taken together, these results indicate that the 3-month intervention with MDCF-2 in 12-18-month-old Bangladeshi children with MAM improved ponderal and linear growth and produced increases in the levels of a group of plasma biomarkers/ mediators of growth and CNS development that were evident for at least 6 months after cessation of treatment.

Discussion

In this study, we performed a two-year follow-up of a cohort of 12-18-month-old Bangladeshi children who had been treated for moderate acute malnutrition (MAM) for 3 months with either a microbiota-directed complementary food (MDCF-2), or a standard ready-to-use supplementary food (RUSF)[25]. We assessed their anthropometric recovery and quantified changes in the representation of >800 bacterial strains (MAGs) present in their fecal microbial communities, plus levels of plasma proteins during the follow-up period. WLZ scores, which were significantly improved by MDCF-2 compared to RUSF at the end of treatment, remained higher in the MDCF-2 group during follow-up. Moreover, despite there being no significant differences in LAZ between the groups at the end of the 3-month intervention, there was a significant difference between the groups during follow-up; namely, the rate of decline in LAZ, which is commonly seen in children in the first few years of life in resource-poor countries in South Asia and Africa[4,5], was significantly less in children who had received MDCF-2 in the antecedent treatment phase. There were no significant differences in diet quality or enteropathogen burden between the treatment groups during the follow-up period. We identified a number of MAGs that were correlated with LAZ after cessation of the intervention,

including strains capable of fermenting dietary glycans to short chain fatty acids. Moreover, several MAGs belonging to Lachnospiraceae, Ruminococcaceae and Oscillospiraceae were linked to both WLZ during treatment and LAZ during follow-up.

The improved linear growth in MDCF-2-treated children in the follow-up period was associated with elevated levels of a group of 37 plasma proteins that persisted for at least 6 months after cessation of treatment; these proteins were previously identified as being positively correlated with WLZ during the treatment phase of the study[25]; their functions are linked to various facets of healthy growth, including musculoskeletal development, central nervous system development and cell growth/proliferation. This set of plasma proteins represent candidate 'leading indicators' of linear growth recovery in undernourished Bangladeshi children. Moreover, they provide a rationale for including more specific clinical measurements beyond anthropometry to more comprehensively characterize physiologic responses to MDCF-2; for example, musculoskeletal and cognitive development which may be manifest over longer time frames than changes in WLZ (or LAZ).

There is a paucity of sufficiently powered longitudinal studies and randomized controlled trials that incorporate detailed characterization of the functional capacity of the microbiome, such as shotgun sequencing of fecal DNA to define changes in the representation of MAGs, and microbial RNA-Seq to relate the expression of metabolic pathways and their products to clinical outcomes. One recent example of the importance of this kind of approach employed a metagenomic analysis of fecal samples from 335 infants/young children living in rural Zimbabwe where there is a high prevalence of stunting. This study revealed that genomic features of the fecal microbial community, in particular, the representation carbohydrate degradation pathways (rather than taxonomic representation), were predictive of linear growth of children during the period of complementary feeding[52]. This finding is consistent with our own studies of growth responses to MDCF-2 in children with MAM; namely that improvements in ponderal growth are driven by specific strains (MAGs) of *P. copri* that express the appropriate repertoire of carbohydrate active enzymes (CAZymes) required to utilize MDCF-2 glycans[28]. Additional studies incorporating similar types of analyses (microbial gene expression, fecal metabolomics) will be required to characterize the *functional* maturation of the microbiota, as well as the relationship between changes in functional activity that link responses to MDCF-2 with linear growth outcomes (including the durability of changes in metabolic activities both during and following intervention).

Our study was relatively small (124 children with MAM enrolled) and the duration of intervention was short (3 months). Moreover, it was not designed to investigate stunting as a primary outcome[24,25]. It will be important to perform larger, longer controlled studies in Bangladesh, as well as in different geographic/sociodemographic settings, to (i) examine the generalizability of the effects of MDCF-2 on stunting without concurrent wasting, versus when both are present in the same child, and (ii) assess the impact of timing (i.e., chronologic age) of initiation of intervention based on the

representation of target MAGs in childrens' gut microbial communities - a process that could be guided by affordable point-of-care diagnostic approaches (e.g., qPCR assays of growth-discriminatory MAGs). In addition, it is important to consider and optimize the dose of the MDCF-2 formulation – especially its constituent glycans - and the duration of treatment. Moreover, the background diet consumed by children may have a significant impact on their growth; based on data from food frequency questionnaires, we had previously found that children who consumed more of the complementary food types present in MDCF-2 in their normal diets during the intervention were more likely to be in the upper quartile of improved weight gain (WLZ)[25].

Taken together, our findings suggest that the effects of MDCF-2 on the gut microbiota of undernourished Bangladeshi children extend beyond weight gain to include improvements in linear growth. Dissecting the mechanistic underpinnings of the effects of the microbial community on growth requires additional research. For example, preclinical studies conducted in gnotobiotic mice colonized with defined communities of cultured, genome-sequenced bacteria corresponding to WLZ- and/or LAZ-associated MAGs represent one approach for dissecting the contributions of MDCF-2 responsive organisms to host pathways involved in ponderal and linear growth as well as other aspects of development, including neurodevelopment. A precedent for such an approach has been established. By combining analyses of microbial community assembly, microbial gene expression and metabolism of glycan constituents of MDCF-2 with single nucleus RNA-Seq and mass spectrometric analyses of the intestine we have confirmed the key role played by specific *P. copri* strains in metabolizing MDCF-2 glycans, promoting weight gain, and stimulating the activities of metabolic pathways involved in lipid, amino acid, carbohydrate plus other facets of energy metabolism in intestinal epithelial cells[53]. A similar strategy should now be employed to examine the role of cultured representatives of the LAZ-associated MAGs identified in the current study on different aspects of linear growth, including accretion of lean body mass, bone development, and maturation of the epiphyseal plates.

References

1. Black RE, Allen LH, Bhutta ZA, et al. Maternal and Child Undernutrition Study Group. Maternal and child undernutrition: global and regional exposures and health consequences. *Lancet* 2008; **371**: 243-60.

2. World Health Organization. WHO child growth standards: growth velocity based on weight, length and head circumference: methods and development (2009). https://www.who.int/publications/i/item/9789241547635

3. United Nations Children's Fund (UNICEF), World Health Organization (WHO), International Bank for Reconstruction and Development/The World Bank. Levels and trends in child

malnutrition: UNICEF / WHO / World Bank Group Joint Child Malnutrition Estimates: Key findings of the 2023 edition. New York: UNICEF and WHO. 2023.

4. de Onis, M., and Branca, F. Childhood stunting: a global perspective. *Maternal & Child Nutrition* 12: 12–26.
5. de Onis M, Borghi E, Arimond M, et al. Prevalence thresholds for wasting, overweight and stunting in children under 5 years. *Public Health Nutrition* 2019; **22**:1–5.
6. Kumar P, Rashmi R, Muhammad T, Srivastava S. Factors contributing to the reduction in childhood stunting in Bangladesh: a pooled data analysis from the Bangladesh demographic and health surveys of 2004 and 2017–18. *BMC Public Health* 2021; **21**: 2101.
7. Victora CG, Adair L, Fall C, et al. for the Maternal and Child Undernutrition Group. Maternal and child undernutrition: consequences for adult health and human capital. *Lancet* 2008; **371**: 340-357.
8. Dewey KG, Begum K. Long-term consequences of stunting in early life. *Matern Child Nutr*. 2011; Suppl **3**: 5-18.
9. Cichon B, Das JK, Salam RA, et al. Effectiveness of Dietary Management for Moderate Wasting among Children > 6 Months of Age-A Systematic Review and Meta-Analysis Exploring Different Types, Quantities, and Durations. *Nutrients* 2023; **15**: 1076.
10. WHO. Guideline: Updates on the Management of Severe Acute Malnutrition in Infants and Children. World Health Organization; Geneva, Switzerland: 2013. PMID: 24649519.
11. Budge S, Parker AH, Hutchings PT, Garbutt C. Environmental enteric dysfunction and child stunting. *Nutr Rev*. 2019; **77**: 240–53.
12. Dewey KG. Reducing stunting by improving maternal, infant and young child nutrition in regions such as South Asia: evidence, challenges and opportunities. *Matern Child Nutr*. 2016; **12** Suppl 1: 27-38.
13. Goudet SM, Bogin BA, Madise NJ, Griffiths PL. Nutritional interventions for preventing stunting in children (birth to 59 months) living in urban slums in low- and middle-income countries (LMIC). *Cochrane Database Syst Rev*. 2019; **6**: CD011695.
14. Odei Obeng-Amoako GA, Wamani H, Conkle J, et al. Concurrently wasted and stunted 6-59 months children admitted to the outpatient therapeutic feeding programme in Karamoja, Uganda: Prevalence, characteristics, treatment outcomes and response. *PLoS One* 2020; **15**: e0230480.
15. Isanaka S, Hitchings MDT, Berthé F, Briend A, Grais RF. Linear growth faltering and the role of weight attainment: Prospective analysis of young children recovering from severe wasting in Niger. *Matern Child Nutr*. 2019; **15**: e12817.
16. Thurstans S, Sessions N, Dolan C, et al. The relationship between wasting and stunting in young children: A systematic review. *Matern Child Nutr*. 2022; **18**: e13246.

17. Dewey KG, Hawck MG, Brown KH, Lartey A, Cohen RJ, Peerson JM. Infant weight-for-length is positively associated with subsequent linear growth across four different populations. *Matern Child Nutr.* 2005; **1**: 11-20.

18. Maleta K, Virtanen SM, Espo M, Kulmala T, Ashorn P. Seasonality of growth and the relationship between weight and height gain in children under three years of age in rural Malawi. *Acta Paediatr*. 2003; **92**: 491-7.

19. Subramanian S, Huq S, Yatsunenko T, et al. Persistent gut microbiota immaturity in malnourished Bangladeshi children. *Nature* 2014; **510**: 417-21.

20. Barratt MJ, Ahmed T, Gordon JI. Gut microbiome development and childhood undernutrition. *Cell Host & Microbe* 2022; **30**: 617-626.

21. Raman AS, Gehrig JL, Venkatesh S, et al. A sparse covarying unit that describes healthy and impaired human gut microbiota development. *Science* 2019; **365**: eaau4735.

22. Blanton LV, Charbonneau MR, Salih T, et al. Gut bacteria that prevent growth impairments transmitted by microbiota from malnourished children. *Science* 2016; **351**: aad3311.

23. Gehrig JL, Venkatesh S, Chang HW, et al. Effects of microbiota-directed foods in gnotobiotic animals and undernourished children. *Science* 2019; **365**: eaau4732.

24. Mostafa I, Nahar N, Islam MM, et al. Proof-of-concept study of the efficacy of a microbiota-directed complementary food formulation (MDCF) for treating moderate acute malnutrition. *BMC Public Health* 2020; **20**: 242.

25. Chen RY, Mostafa I, Hibberd MC, et al. A Microbiota-Directed Food Intervention for Undernourished Children. *N Engl J Med*. 2021; **384**: 1517-1528.

26. Liu J, Platts-Mills JA, Juma J, et al. Use of quantitative molecular diagnostic methods to identify causes of diarrhoea in children: a reanalysis of the GEMS case-control study. *Lancet* 2016; **388**: 1291–1301.

27. Platts-Mills JA, Liu J, Rogawski ET, et al. Use of quantitative molecular diagnostic methods to assess the aetiology, burden, and clinical characteristics of diarrhoea in children in low-resource settings: a reanalysis of the MAL-ED cohort study. *Lancet Glob. Health* 2018; **6**: e1309–e1318.

28. Hibberd MC, Webber DM, Rodionov DA, et al. Bioactive glycans in a microbiome-directed food for malnourished children. *Nature* 2024; **625**: 157-165.

29. Benjamini Y and Hochberg Y. Controlling the false discovery rate: a practical and powerful approach to multiple testing. *J R Stat Soc Series B Stat Methodol.* 1995; **57**: 289-300.

30. Baym M, Kryazhimskiy S, Lieberman TD, Chung H, Desai MM, Kishony R. Inexpensive multiplexed library preparation for megabase-sized genomes. *PLoS One* 2015; **10**: e0128036.

31. Bray NL, Pimentel H, Melsted P, Pachter L. Near-optimal probabilistic RNA-seq quantification. *Nat Biotechnol*. 2016; **34**: 525-7.

680 32. Wood DE, Lu J, Langmead B. Improved metagenomic analysis with Kraken 2. *Genome Biol*.
681 2019; **20**: 257.
682 33. Lu J, Breitwieser FP, Thielen P, and Salzberg S. Bracken: estimating species abundance in
683 metagenomics data. *PeerJ. Computer Science* 2017; **3:** e104.
684 34. Chaumeil PA, Mussig AJ, Hugenholtz P, Parks DH. GTDB-Tk: a toolkit to classify genomes with
685 the Genome Taxonomy Database. *Bioinformatics* 2019; **36**: 1925–7.
686 35. Hoffman GE and Roussos P. Dream: powerful differential expression analysis for repeated
687 measures designs. *Bioinformatics* 2020; **37:** 192–201.
688 36. Korotkevich G, Sukho V, Budin N, et al., Fast gene set enrichment analysis. *bioRxiv* 2021;
689 https://doi.org/10.1101/060012.
690 37. Love, M.I., Huber, W. and Anders, S. Moderated estimation of fold change and dispersion for
691 RNA-seq data with DESeq2. *Genome Biol*. 2014; **15**: 550.
692 38. Indicators for assessing infant and young child feeding practices: definitions and measurement
693 methods. Geneva: World Health Organization and the United Nations Children's Fund
694 (UNICEF), 2021.
695 39. Duncan, S. H., Barcenilla, A., Stewart, C. S., Pryde, S. E., and Flint, H. J. Acetate utilization and
696 butyryl coenzyme A (CoA):acetate-CoA transferase in butyrate-producing bacteria from the
697 human large intestine. *Appl. Environ. Microbiol.* 2002; **68**: 5186–5190.
698 40. Durand GA, Pham T, Ndongo S, et al. *Blautia massiliensis* sp. nov., isolated from a fresh human
699 fecal sample and emended description of the genus *Blautia*. *Anaerobe* 2017; **43**: 47-55.
700 41. Hou X, Wu N, Ren S, et al. Profiling *Blautia* at high taxonomic resolution reveals correlations
701 with cognitive dysfunction in Chinese children with Down syndrome. *Front Cell Infect Microbiol.*
702 2023; **13**: 1109889.
703 42. Cole F, Zhang W, Geyra A, Kang JS, Krauss R.S. Positive regulation of myogenic bHLH factors
704 and skeletal muscle development by the cell surface receptor CDO. *Dev Cell* 2004; **7**: 843–854.
705 43. Takeda U, Utani A, Wu J, et al. Targeted disruption of dermatopontin causes abnormal collagen
706 fibrillogenesis. *J Invest Dermatol*. 2002; **119**: 678-83.
707 44. Hankenson KD, Hormuzdi SG, Meganck JA, Bornstein P. Mice with a disruption of the
708 thrombospondin 3 gene differ in geometric and biomechanical properties of bone and have
709 accelerated development of the femoral head. *Mol Cell Biol.* 2005; **25**: 5599-606.
710 45. Stenina-Adognravi O, Plow EF. Thrombospondin-4 in tissue remodeling. *Matrix Biol.* 2019; **75-**
711 **76**: 300-313.

712 46. David A, Hwa V, Metherell LA, et al. Evidence for a continuum of genetic, phenotypic, and
713 biochemical abnormalities in children with growth hormone insensitivity. *Endocr Rev*. 2011; **32**:
714 472-97.

715 47. Kiper POS, Saito H, Gori F, et al. Cortical-Bone Fragility--Insights from sFRP4 Deficiency in
716 Pyle's Disease. *N Engl J Med.* 2016; **374**: 2553-2562.

717 48. Baloh RH, Enomoto H, Johnson EM Jr, Milbrandt J. The GDNF family ligands and receptors -
718 implications for neural development. *Curr Opin Neurobiol.* 2000; **10**: 103-10.

719 49. Liu Y, Zhang L, Mei R, et al. The Role of SliTrk5 in Central Nervous System. *Biomed Res Int.*
720 2022; 4678026.

721 50. Park H, Poo MM. Neurotrophin regulation of neural circuit development and function. *Nature*
722 *Reviews Neuroscience.* 2013; **14**: 7–23.

723 51. Yuan N, Wang X, He M. Robo2 promotes osteoblast differentiation and mineralization through
724 autophagy and is activated by parathyroid hormone induction. *Ann Anat.* 2023; **248**: 152070.

725 52. Robertson RC, Edens TJ, Carr L, et al. The gut microbiome and early-life growth in a population
726 with high prevalence of stunting. *Nat Commun*. 2023; **14**: 654.

727 53. Chang HW, Lee EM, Wang Y, et al. Prevotella copri and microbiota members mediate the
728 beneficial effects of a therapeutic food for malnutrition. *Nat Microbiol*. 2024; **9**: 922-937

Contributors

I.M., with assistance from H.H.R., M.M., T.H. conducted the long-term follow-up for the clinical trial and collected anthropometry and clinical metadata. I.M., M.C.H. and M.J.B. analyzed dietary data and anthropometry as reported in Figure 1 and Tables 1 and 2. M.C.H. analyzed the enteropathogen qPCR data, mapped shotgun sequencing data to MAGs and conducted analyses of MAG abundance associations with prior MDCF-2 treatment and/or anthropometry that are reported in Figure 2. S.J.H. analyzed the correlations between plasma protein levels and LAZ or WLZ scores reported in Figure 3. M.J.B. oversaw databases of clinical metadata and the biospecimen archive. T.A. and J.I.G. supervised this research project. I.M., M.J.B. M.C.H. and J.I.G. wrote the paper with invaluable input from co-authors.

Data sharing

The data supporting the findings of this study are available within the supplementary materials; shotgun sequencing data in raw format (prior to post-processing and data analysis) have been deposited at the European Nucleotide Archive (ENA) under study accession PRJEB66487.

Declaration of interests

The authors declare no competing interests.

Acknowledgments:

We are grateful to the families of study participants and icddr,b investigators and staff for their contributions to the collection of biospecimens and data reported here. We appreciate the support of the Bill and Melinda Gates Foundation and the Governments of Bangladesh and Canada for providing core/unrestricted support to icddr,b. We thank Su Deng, Kazi Ahsan, Martin Meier, Jessica Hoisington-Lopez, and MariaLynn Crosby for their technical assistance with processing biospecimens. The support of members of the Genome Technology Access Core (GTAC) at Washington University School of Medicine in shotgun sequencing of fecal DNA and enteropathogen qPCR is greatly appreciated.

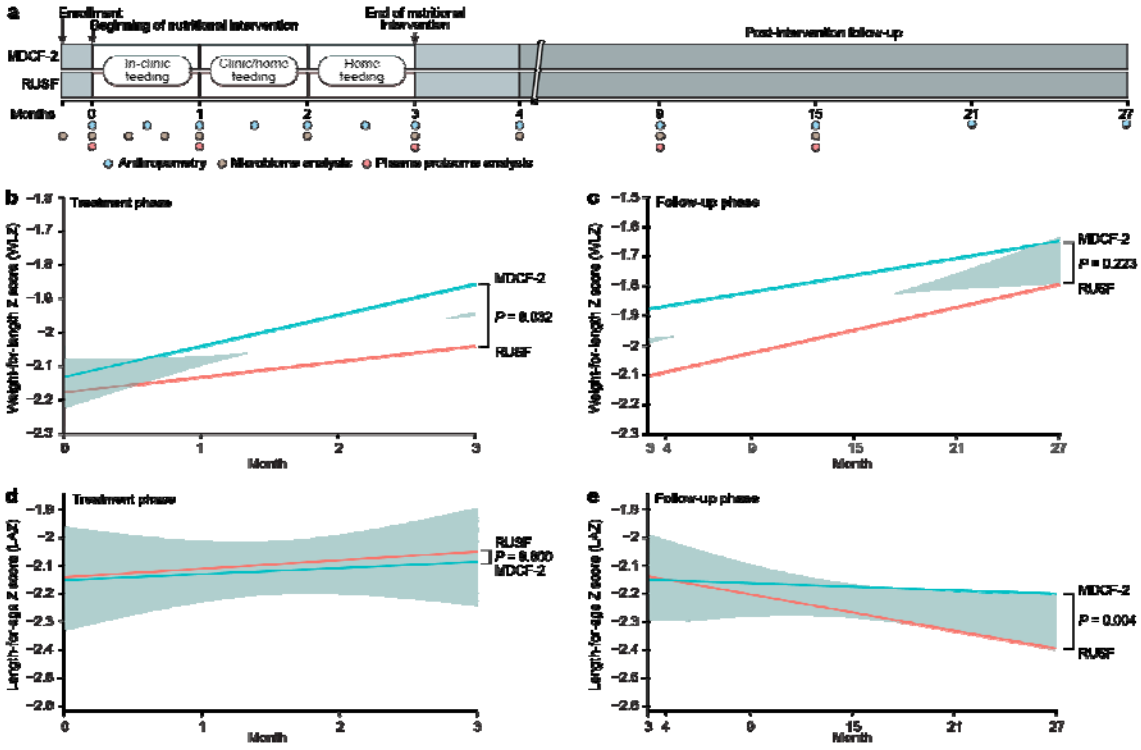

Figure 1. Anthropometric trajectories during treatment with MDCF-2 or RUSF and during the two year post-intervention follow-up period. (**a**) Trial design, including timing of biospecimen collection for analysis of the microbiome and plasma proteome. (**b,c**) Weight-for-length Z-score (WLZ) trajectories during the three months of MDCF-2 or RUSF treatment (panel b) and during the two years of post-intervention follow-up (panel c). (**d,e**) Length-for-age Z-score (LAZ) trajectories during the three months of MDCF-2 versus RUSF treatment phase of the trial (panel d) or the two years of post-intervention follow-up (panel e). Each plot indicates a simple linear fit of the data for the MDCF-2 (blue) and RUSF (red) treatment groups along with the 95% confidence interval. The linear, mixed effects model for each anthropometric assessment (Eq. 2; *Methods*) was used to determine the coefficient (β) and statistical significance (*P*) for the specified effect. For the treatment phase analysis, the beginning of nutritional intervention was used at the baseline measurement, whereas for the follow-up analysis, the baseline used was the end of 3-month nutritional intervention.

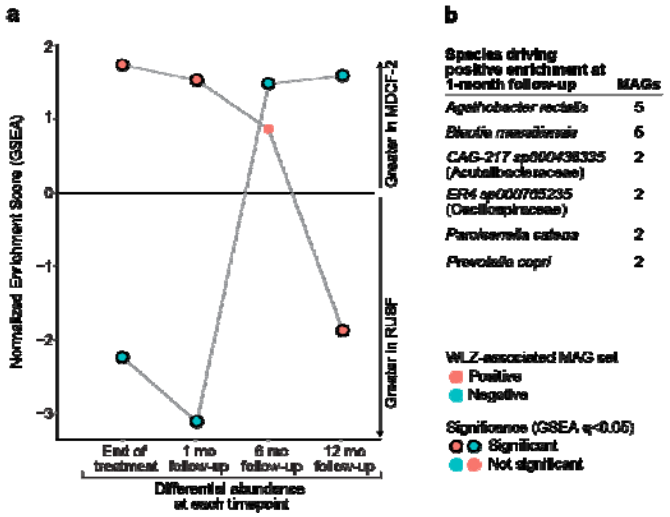

Figure 2. Differences in bacterial MAG abundances between fecal samples collected from MDCF-2- and RUSF-treated trial participants during the post-intervention follow-up. (a) The enrichment of groups of positively (red) or negatively (blue) WLZ-associated MAGs after ranking by differential abundance between the MDCF-2 or RUSF groups at end of treatment and at the 1-, 6-, or 12- month post-intervention time points. Normalized Enrichment Scores (NES) were determined by GSEA. Points representing significant NES significant ($q<0.05$) are outlined in black. (**b**) Taxonomic assignments of MAGs driving the enrichment of positively WLZ-associated MAGs in the analysis depicted in (a). Species assignments are shown for taxa containing >1 MAG.

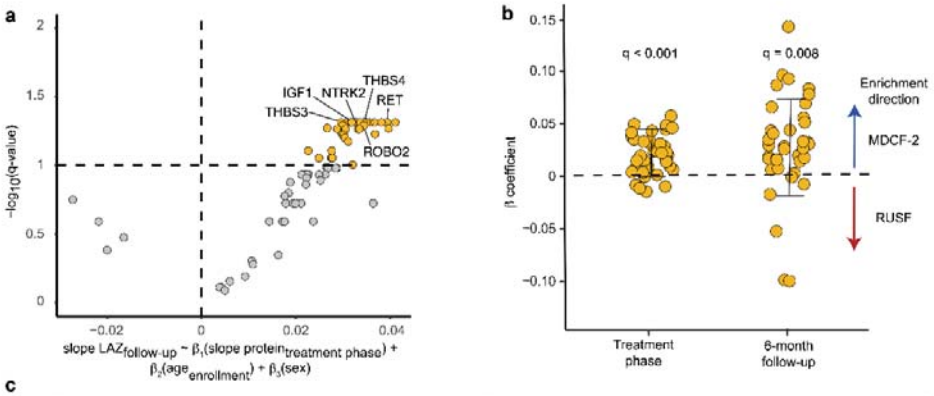

c

Protein ID	Name	Functional annotation
Connective tissue/musculoskeletal and organ development		
CDON	Cell adhesion molecule-related/down-regulated by oncogenes	Regulation of myogenesis
CILP2	Cartilage intermediate layer protein 2	Mediates collagen interactions within articular cartilage matrices
COL15A1	Collagen alpha-1(XV) chain	Structural support in connective tissues
COL28A1	Collagen alpha-1(XXVIII) chain	Promotes proliferation and migration in renal cells
COL6A3	Collagen alpha-3(VI) chain	Stabilizes collagen VI chains
COL9A1	Collagen alpha-1(IX) chain	Structural support in connective tissues
DPT	Dermatopontin	Extracellular matrix structure
FAP	Prolyl endopeptidase FAP	Tissue remodeling, fibrosis, and wound healing
HAPLN1	Hyaluronan and proteoglycan link protein 1	Stabilization of extracellular matrix
IGDCC4	Immunoglobulin superfamily DCC subclass member 4	Cell-cell adhesion
LRRC15	Leucine-rich repeat-containing protein 15	Involved in collagen and fibronectin binding
OLFM2	Noelin-2	Regulates gene expression in smooth muscle cells
SCIN	Adseverin	Actin binding protein, regulates chondrocyte activity
THBS3	Thrombospondin-3	Cellular remodeling and membrane stability
THBS4	Thrombospondin-4	Tissue remodeling, wound healing
CNS/Neuronal function		
DCLK1	Serine/threonine-protein kinase DCLK1	Neuron migration, apoptosis and neurogenesis
FLRT2	Leucine-rich repeat transmembrane protein FLRT2	Regulation of synapse assembly and neuron migration
LRRC4C	Leucine-rich repeat-containing protein 4C	Binds to netrin G1 axon guidance molecule
NTRK2	BDNF/NT-3 growth factors receptor	Synaptogenesis and neuronal development; role in learning and memory
ROBO2	Roundabout homolog 2	Axon guidance and cell migration
ROR1	Inactive tyrosine-protein kinase transmembrane receptor ROR1	Modulates neurite growth
SLITRK5	SLIT and NTRK-like protein 5	Regulation of CNS development
Cell growth /proliferation		
CRABP2	Cellular retinoic acid-binding protein 2	Facilitates internalization of retinoic acid
IGF1	Insulin-like growth factor I	Regulation of cell growth, proliferation, and survival
IL11RA	Interleukin-11 receptor subunit alpha	Supports proliferation of hematopoietic stem cells
MFAP2	Microfibrillar-associated protein 2	Control of growth factor signal transduction
PPIC	Peptidyl-prolyl cis-trans isomerase C	Facilitates protein folding
PXDN	Peroxidasin homolog	Promotes angiogenesis and modulates ERK1/2,Akt and FAK signaling
RET	Proto-oncogene tyrosine-protein kinase receptor Ret	Regulation of proliferation and organ development
SFRP4	Secreted frizzled-related protein 4	Modulator of Wnt signaling
SMOC2	SPARC-related modular calcium-binding protein 2	Wound healing, endothelial cell proliferation
Complement system		
C1QTNF3	Complement C1q tumor necrosis factor-related protein 3	Adipokine, anti-inflammatory, promotion of angiogenesis
CD93	Complement component C1q receptor	Complement activation
Other		
CDH5	Cadherin-5	Assembly and maintenance of endothelial adherens junction
COLEC12	Collectin-12	Recognition of microbial cell wall components
LYVE1	Lymphatic vessel endothelial hyaluronic acid receptor 1	Involvement in lymphatic hyaluronan transport and uptake
SCARF2	Scavenger receptor class F member 2	Binding and degradation of acetylated low density lipoprotein

Fig 3 - Effects of MDCF-2 on the plasma proteome of children with MAM during nutritional intervention and in the follow-up period. (a) Volcano plot of WLZ-associated plasma proteins that are also associated with LAZ responses during the post-treatment follow-up period. The linear model described under the plot was applied to relate the rate of change for each participant in the levels of proteins during the treatment-phase to the rate of change of LAZ during the follow-up. Significant LAZ-predictive proteins (q<0.1) are colored in orange. (**b**) Annotated functions of the 37 plasma proteins associated with the effect of MDCF-2 on LAZ during the follow-up period. (**c**) Association of the 37 proteins with treatment arm during the 3-month treatment phase and at the 6-month follow-up time point. One-way t-tests were applied to the β3 coefficient in Eq. 9 and the β1 coefficient in Eq. 10 (see *Methods*, q<0.05) at each time point to test the statistical significance of their enrichment in either the MDCF-2 or RUSF treatment arm.

Characteristic	MDCF-2	RUSF	β_1(treatment group)†	*P*-value†
	mean ± SD			
Number of participants	59	59		
Age at completion of intervention (mo.)	18.6 ± 1.92	18.9 ± 1.94	-0.155	0.662
Sex - Female (percent)‡	34 (58)	33 (56)		1
WLZ	-1.88 ± 0.56	-2.13 ± 0.62	0.255	**0.022**
WAZ	-2.39 ± 0.70	-2.56 ± 0.72	0.15	0.252
LAZ	-2.08 ± 1.08	-2.06 ± 1.02	-0.065	0.737
MUAC (cm)	13.2 ± 0.48	13.1 ± 0.46	0.117	0.162
Weight (kg)	7.99 ± 0.77	8.10 ± 0.72	0.143	0.241
Length (cm)	76.3 ± 3.2	76.0 ± 3.4	-0.133	0.813

Table 1: Anthropometric characteristics of children in each study arm at the end of the 3-month intervention (beginning of follow-up phase). † Model: anthropometry ~ β_1(treatment group) + β_2(age at baseline) + β_3(sex) + β_4(illness in prior 7 days). Note that the 'age at baseline' term was omitted when 'age at baseline' was tested. ‡ Fisher's Exact Test.

Months of follow-up after intervention	MDCF-2 (n=59)	RUSF (n=59)	Difference (95% CI)
	LAZ (mean ± SD)		
1	-2.09 ± 1.07	-2.09 ± 1.00	-
6	-2.28 ± 1.00	-2.31 ± 0.92	0.03 (-0.32, 0.39)
12	-2.24 ± 0.93	-2.42 ± 0.86	0.18 (-0.16, 0.52)
18	-2.26 ± 0.96	-2.42 ± 0.87	0.16 (-0.18, 0.51)
24	-2.09 ± 0.92	-2.22 ± 0.80	0.13 (-0.20, 0.46)

Table 2: LAZ scores of participants in each study arm during the 24-month follow-up period.

796 **List of Supplementary Materials**

797 **Supplementary Table S1.** Analyses of anthropometry data

798 **Supplementary Table S2:** Analysis of enteropathogen abundances

799 **Supplementary Table S3:** Analysis of metagenome-assembled genome (MAG) abundances

800 **Supplementary Table S4.** Plasma protein levels related to anthropometric responses and treatment

801